HHS Public Access

Author manuscript

Biol Psychiatry. Author manuscript; available in PMC 2018 February 01.

Published in final edited form as:

Biol Psychiatry. 2017 February 01; 81(3): 193–202. doi:10.1016/j.biopsych.2016.06.008.

SOCIABILITY DEFICITS AND ALTERED AMYGDALA CIRCUITS IN MICE LACKING *Pcdh10*, AN AUTISM ASSOCIATED GENE

Hannah Schoch[1,*], **Arati S. Kreibich**[2,*], **Sarah L. Ferri**[8], **Rachel S. White**[2], **Dominique Bohorquez**[2], **Anamika Banerjee**[2], **Russell G. Port**[2], **Holly C. Dow**[2], **Lucero Cordero**[2], **Ashley A. Pallathra**[2], **Hyong Kim**[2], **Honghze Li**[3], **Warren B. Bilker**[3], **Shinji Hirano**[4], **Robert T. Schultz**[5], **Karin Borgmann-Winter**[2,9], **Chang-Gyu Hahn**[2], **Dirk Feldmeyer**[6,7], **Gregory C. Carlson**[2], **Ted Abel**[8], and **Edward S. Brodkin**[2]

[1]Cell and Molecular Biology Graduate Group, Perelman School of Medicine at the University of Pennsylvania, Smilow Center for Translational Research, Room 10-170, Building 421, 3400 Civic Center Boulevard, Philadelphia, PA 19104-6168, USA

[2]Center for Neurobiology and Behavior, Department of Psychiatry, Perelman School of Medicine at the University of Pennsylvania, Translational Research Laboratory, 125 South 31st Street, Room 2220, Philadelphia, PA 19104-3403, USA

[3]Department of Biostatistics and Epidemiology, Perelman School of Medicine at the University of Pennsylvania, 215 Blockley Hall, 423 Guardian Drive, Philadelphia, PA 19104-6021, USA

[4]Department of Cell Biology, Kansai Medical University, 2-5-1 Shinmachi, Hirakata City, Osaka 573-1010, Japan

[5]Center for Autism Research, Children's Hospital of Philadelphia, and Departments of Pediatrics and Psychiatry, Perelman School of Medicine, University of Pennsylvania, 3535 Market Street, Philadelphia, PA 19104, USA

[6]Forschungzentrum Julich, Institute of Neuroscience and Medicine, INM-2, D-52425, Julich, Germany

[7]RWTH Aachen University, Medical School, Department of Psychiatry, Psychotherapy and Psychosomatics, D-52074 Aachen, Germany

[8]Department of Biology, University of Pennsylvania, Smilow Center for Translational Research, Room 10-133, Building 421, 3400 Civic Center Boulevard, Philadelphia, PA 19104-6168, USA

Corresponding Author: Edward S. Brodkin, tel (215)-746-0118; fax: (215)-573-2041; ebrodkin@mail.med.upenn.edu.

*These authors contributed equally

Financial Disclosures

Warren Bilker has consulted for Janssen Pharmaceuticals. The consulting is not related to the subject matter of the manuscript. Robert T. Schultz has received consulting fees from Akili Inc, Johnson & Johnson Consumer Inc, and Lumos Pharma Inc. The consulting is not related to the subject matter of the manuscript. All other authors report no biomedical financial interests or potential conflicts of interest.

[9]Department of Child and Adolescent Psychiatry, Children's Hospital of Philadelphia, Philadelphia, PA 19104, USA

Abstract

Background—Behavioral symptoms in individuals with autism spectrum disorder (ASD) have been attributed to abnormal neuronal connectivity, but the molecular bases of these behavioral and brain phenotypes are largely unknown. Human genetic studies have implicated *Protocadherin 10 (PCDH10)*, a member of the δ2 subfamily of non-clustered protocadherin genes, in ASD. PCDH10 expression is enriched in the basolateral amygdala, a brain region implicated in the social deficits of ASD. Previous reports indicate that *Pcdh10* plays a role in axon outgrowth and glutamatergic synapse elimination, but its roles in social behaviors and amygdala neuronal connectivity are unknown. We hypothesized that haploinsufficiency of *Pcdh10* would reduce social approach behavior and alter the structure and function of amygdala circuits.

Methods—Mice lacking one copy of *Pcdh10* (*Pcdh10*$^{+/-}$) and wildtype littermates (WT) were assessed for social approach and other behaviors. The lateral/basolateral amygdala was assessed for dendritic spine number and morphology, and amygdala circuit function was studied using voltage sensitive dye imaging. Expression of Pcdh10 and N-methyl-D-aspartate receptor (NMDAR) subunits was assessed in post-synaptic density fractions of amygdala.

Results—Male *Pcdh10*$^{+/-}$ mice have reduced social approach behavior, as well as impaired gamma synchronization, abnormal spine morphology, and reduced levels of NMDAR subunits in amygdala. Social approach deficits in *Pcdh10*$^{+/-}$ males were rescued with acute treatment with the NMDAR partial agonist d-cycloserine.

Conclusions—Our studies reveal that male *Pcdh10*$^{+/-}$ mice have synaptic and behavioral deficits, and establish *Pcdh10*$^{+/-}$ mice as a novel genetic model for investigating neural circuitry and behavioral changes relevant to ASD.

Keywords

protocadherin; gene; amygdala; synapse; NMDA; autism

Introduction

Reduced sociability, or the tendency to seek out and engage in social interactions, is a highly disabling and treatment-refractory core feature of autism spectrum disorders (ASD) (1). Epidemiological studies of ASD consistently indicate that it is more common in males than females; however, the biological bases of male predominance in ASD are poorly understood (2,3). Multiple lines of evidence point to abnormal development and maintenance of synaptic connections as key neurobiological features of ASD (4–7). Human linkage studies have identified multiple ASD-associated genes that are implicated in the structure and function of neuronal synapses (4,8–10) including the cadherin and protocadherin superfamily of calcium-dependent neural cell adhesion molecules (9,11,12). Copy number variants of the Protocadherin 10 (*PCDH10*) gene and its regulatory region have been associated with ASD, suggesting that it may play a role in the pathophysiology of the disorder (9,13).

Pcdh10 (*OL-protocadherin*) is a member of the δ2 subfamily of non-clustered protocadherins (12) that is enriched in the mammalian brain (14). *Pcdh10* is an activity-regulated gene on murine chromosome 3 that is expressed at high levels in olfactory and limbic regions, including the basolateral amygdala, which is implicated in social and emotional behavior phenotypes in ASD (14–16). In neurons, Pcdh10 functions in a molecular pathway with Fragile X mental retardation protein (FMRP) and myocyte enhancer factor 2 (MEF2) to regulate the stability of the post-synaptic density following neuronal activity (17). FMRP binds *Pcdh10* mRNA transcripts and transports them to the synapse (17,18). At the synapse, Pcdh10 has been linked to both spinogenesis and synapse elimination. A synaptic transmembrane protein, Pcdh10 interacts with Nck-associated protein 1 (Nap1) to recruit the WAVE actin polymerization complex, a mechanism linked to lamellipodia extension and spinogenesis (19–21). Following neuronal activity, Pcdh10 facilitates proteosomal degradation of postsynaptic density protein 95 (PSD-95) and is required for MEF2-induced synapse elimination (17).

Here, we use a mutant mouse model to investigate the role of *Pcdh10* in modulating sociability, as well as amygdala structural and functional connectivity, phenotypes relevant to ASD. We demonstrate a role for *Pcdh10* as a regulator of sociability, and a modulator of synaptic function in the amygdala.

Methods and Materials

Animal Housing

All mice were cared for in accordance with the National Academy of Sciences Guide for the Care and Use of Laboratory Animals and all animal procedures were approved by the University of Pennsylvania Institutional Animal Care and Use Committee (IACUC). $Pcdh10^{+/-}$ mice in which the first exon of *Pcdh10* had been replaced with a *lacZ-neo* selection cassette were produced by Lexicon Pharmaceuticals, Inc. (USA) (22). Founders were backcrossed to a C57BL/6N genetic background for more than 15 generations (personal communication from Shinji Hirano). Male $Pcdh10^{+/-}$ mice were crossed with female C57BL/6J (B6) mice, to generate wild-type (WT, $Pcdh10^{+/+}$) or heterozygous null ($Pcdh10^{+/-}$) experimental animals. Experimental subjects were the offspring of at least two consecutive backcrosses to C57BL/6J. Same-sex littermates were group-housed with 2 – 5 per cage in a temperature and humidity controlled environment in a 12-hour light-dark cycle. All mice had access to food and water *ad libitum*. Litters were randomly assigned to undergo behavior testing, electrophysiology, dendritic spine, or biochemical analysis. Behavioral testing and tissue collection were conducted during the light phase.

Behavior

Separate cohorts of male and female, $Pcdh10^{+/-}$ and wild-type littermates (WT) underwent different sets of behavioral tests. Cohort 1 consisted of juveniles (28–32-day-old) that underwent the Social Approach Test. A second cohort of $Pcdh10^{+/-}$ and WT mice underwent tests in the following order, starting at 28–32 days of age: olfactory habituation-dishabituation (day 1), elevated zero maze (day 2), and accelerating rotarod (day 3). A third cohort underwent observations of repetitive behaviors (rearing, self-grooming, digging,

circling) in the home cage (see Figure S2). A fourth cohort of juvenile mice underwent the social approach test 30 minutes following intraperitoneal administration of saline or d-cycloserine. A fifth cohort of postnatal day 6 mice pups underwent measurement of ultrasonic vocalizations following separation from the dam and nest. A sixth cohort of adult *Pcdh10*$^{+/-}$ and WT mice underwent the novel object recognition task. Cohort sizes were similar to previously published results (23–26).

Social Approach Test—Naïve mice underwent the Social Approach Test in a darkened behavioral testing room, using methods described previously (23). The Social Approach Test in a 3-chambered apparatus is perhaps the most widely used assay of social interaction used to assess mouse models relevant to autism (27–34), and has been shown to have good reliability and ecological validity (23).

The two end chambers of the 3-chambered testing apparatus each contained an empty, transparent, perforated Plexiglas cylinder. For the initial 10-minute habituation phase, each subject was allowed to freely explore the three chambered apparatus with empty cylinders (*Phase 1*). Immediately following habituation, one cylinder was loaded with a non-social stimulus (paperweight) and the other cylinder with a social stimulus (same-sex adult gonadectomized A/J mouse) and the test mouse was allowed to explore the apparatus and cylinders for 10 minutes (*Phase 2*). Time spent sniffing each cylinder, time spent in each chamber, as well as the distance each test mouse traveled was scored in each Phase, using the automated behavioral analysis system, TopScan (Clever Systems Inc., Reston, VA, USA) (23). A separate cohort of mice was given a single intra-peritoneal injection of saline or 32mg/kg d-cycloserine 30 minutes prior to testing.

Pup ultrasonic vocalizations—Postnatal day 6 (35) male and female pups were separated from their mother and placed alone in a glass container (10 cm × 8 cm × 7 cm; open surface) containing clean bedding, which was placed in an open Styrofoam container (20 cm × 21 cm × 12 cm) inside a sound-attenuating cabinet (Med Associates, St. Albans, VT), for 5 min. Ultrasonic vocalizations were recoded using an UltraSoundGate Condenser Microphone CM 16 (Avisoft Bioacoustics, Berlin, Germany), placed 12 cm above the floor of the sound attenuating box, and an UltraSoundGate 116H audio device (Avisoft Bioacoustics). Recordings were made with Avisoft RECORDER software (version 4.2.14; Avisoft Bioacoustics) using a sampling rate of 375,000 Hz in a 16 bit format. Numbers of USVs emitted over 5 minutes were counted.

Neuronal reconstruction and spine counts

Adult male mice were sacrificed and whole brains were removed, rinsed in PBS, and Golgi impregnation was conducted using the FD Rapid GolgiStain kit (FD Neurotechnologies, Columbia, MD, USA). After 5 days of impregnation in kit solution A/B, brains were placed in solution C twice for 24hrs each. Brains were frozen and 100μm coronal sections were taken on a cryostat. Sections were mounted on gelatin-coated slides, and thoroughly dried at room temperature protected from light over 7 or more days. Slides were developed according to the manufacturer's instructions, and coverslipped using Permount mounting medium (Thermo-Fisher, Waltham, MA). Clearly-stained spiny lateral/basolateral (LA/

BLA) amygdala neurons located between the external and amygdala capsule fiber tracts were manually reconstructed using Neurolucida neuron tracing software (MBF Bioscience, Williston, VT) by an experimenter blinded to genotype. Traced neurons with multiple dendrites over 140 μm in length were selected for spine counts. Proximal (within 100 μm of the soma) and distal (within 100 μm of the terminus) dendritic regions (50 μm length) were identified on long dendrites, and all visible spines within the 50 μm region were manually identified and counted by type (36,37). Spine counts were performed at low focal depth to improve the optical resolution. A maximum of two dendrites, each with a proximal and a distal region were counted on one to two neurons per animal. Average spine counts of each type per 50 μm were calculated for each genotype. Contrast enhancement of representative images was applied equally to each image to increase clarity.

Electrophysiology

Voltage sensitive dye imaging (VSD) experiments were performed according to previous studies (38). 300μm slices from juvenile (28–32 day old) *Pcdh10*$^{+/-}$ and wild-type mice were stained for 15 min with 0.125 mg/ml (in ACSF) of the voltage sensitive dye di-3-ANEPPDHQ (D36801, Invitogen, Carlsbad, CA), and imaged in an oxygenated interface chamber using an 80 × 80 CCD camera recording at a 1 kHz frame rate (NeuroCCD: RedShirtImaging, Decatur, GA). Epi-illumination was provided by a custom LED illuminator. Slices were continuously bathed in ACSF. Single or burst stimulation of 4–40-mA, 200-μs pulses at 40Hz were administered with the electrode placed in the most dorsal region of the lateral amygdala (LA). After initial electrode placement and establishment of slice viability, baseline responses with control ACSF were elicited by either 12 burst stimulus trials, each separated by 40s.

To analyze VSD data, a data processing program was used in IGOR (Wavemetrics, Lake Oswego, OR) to calculate change in fluorescence divided by the resting fluorescence. Regions of Interest (ROI) were chosen according to a standardized anatomy of the amygdala. The ROI for the lateral amygdala excluded the area where the electrode was placed. The basolateral amygdala (BLA) was ventral medial to the LA. The striatum (STR) was selected dorsal medial to the LA. Fluorescence-changes are calculated as the percent change in fluorescence divided by the resting fluorescence (%dF/F0). Colored images were generated in IGOR on 12-trial-averages. For gamma power analysis data was imported into Matlab (Mathworks, Natick, MA), and processed with the open source tool box FieldTrip (39). Time-locked averaged data were transformed to time frequency space using Morlet wavelets (40) to allow calculation of evoked power. To quantify changes in power, the region of the steady-state gamma was observed on the time-frequency plot, and the integral response was calculated using in house scripts.

Sub-cellular fractionation and semi-quantitative western blotting

Adult *Pcdh10*$^{+/-}$ and wild-type male mice were rapidly decapitated and amygdala tissue was collected and flash frozen. 50 mg amygdala (5 animals were pooled into three samples of 50 mgs in each group, transgenic or wild types) were fractionated into various subcellular fractions using methods previously described (41,42). Protein extracts including PSD fractions were size fractionated in 7.5% Tris Glycine (Biorad, Hercules, CA) gels and

western blotted with the following antibodies: PCDH10 (rat OL-protocadherin, clone 5G10, cat# MABT20, Millipore, Billerica, MA); β-actin (mouse, cat# A2228, Sigma, St. Louis, MO); PSD-95 (mouse, cat# 75-028, NeuroMab, Davis, CA); and GLUN1 (goat, cat# sc-1467) GLUN2A (goat, cat# sc-1468), and SRC (mouse, cat# sc-5266), all from Santa Cruz Biotechnology, Dallas, TX). The quantified band intensities were analyzed and plotted using the Graph Pad Prism software; paired two tailed Student's t test was used for between group comparisons.

Data analysis

Sample sizes for experiments were chosen based on adequately powered sample sizes used for the same types of data published by our research group and others (22,39,42–46). No animals were excluded from the analysis of behavior, VSDi, spine analysis, and biochemistry. Investigators were blinded to the genotype of mice during experiments and data collection, but were un-blinded during data analysis. The behavioral and structural data are presented as mean ±SEM. The analyses for most experiments (except electrophysiology experiments and where otherwise noted) were based on a mixed model regression model (47,48) with restricted maximum likelihood, which in this case is analogous to a fixed effects repeated measures ANOVA, but both allows for individual missing data points without imputation, and allows for greater flexibility of the variance structure of the repeated measures. If repeated measures were taken in the same mice (*e.g.*, in Phase 1 and Phase 2 of the Social Approach Test), this was accounted for in the analysis. Analysis of ultrasonic vocalization data and repetitive behavior data was based on a Mixed Effects Poisson model which is used for count data. Analysis of electrophysiology data and the novel object recognition data was based on a Mann-Whitney test (the non-parametric alternative to a two-sample t-test). In some cases, log transformations were applied for outcome variables due to potential non-normality, and those cases are noted in the Figure legends. The threshold for significance was $p<0.05$.

Results

Pcdh10$^{+/-}$ male mice exhibit reduced sociability

We tested male and female juvenile 28–32-day-old *Pcdh10*$^{+/-}$ mice and wild type littermates (WT) in the Social Approach Test (23,49,50) and used social cylinder sniff duration as the primary measure of sociability, because it is the variable in the test with the most reliability and ecological validity (23). Male *Pcdh10*$^{+/-}$ mice showed lower social approach, *i.e*, significantly less increase in social cylinder sniffing duration from Phase 1 (absence of stimulus mouse) to Phase 2 (presence of stimulus mouse) than did male WT littermates (phase by genotype interaction, $p=0.037$). Both genotypes taken together showed a significant increase in sniffing in Phase 2 relative to Phase 1 (main effect of phase, $p=0.001$). There was no significant difference between the genotypes in sniffing time of the social cylinder overall across both phases (no significant main effect of genotype) (Figure 1a). For duration of sniffing the nonsocial cylinder (which was empty in Phase 1 and contained a novel object in Phase 2), there was no significant phase by genotype interaction, main effect of phase, or main effect of genotype (Figure 1b). For distance traveled, there was a significant phase by genotype interaction ($p<0.001$), with a significant main effect of phase

(p<0.001) but no significant main effect of genotype (Figure 1c). In summary, relative to male WT littermates, male *Pcdh10*$^{+/-}$ mice showed significantly reduced social approach but no change in general exploratory activity in this test.

Female *Pcdh10*$^{+/-}$ mice showed no significant difference from female WT in social approach (no significant phase by genotype interaction). Both genotypes taken together showed a significant increase in social cylinder sniffing in Phase 2 relative to Phase 1 (main effect of phase, p=0.001). Taking both phases together, female *Pcdh10*$^{+/-}$ mice sniffed the social cylinder significantly less than female WT littermates (main effect of genotype, p=0.039) (Figure 1d). For nonsocial cylinder sniff duration, there was no significant phase by genotype interaction, but there were significant main effects of phase (p=0.006) and genotype (p=0.022) (Figure 1e). For distance traveled, there was a significant phase by genotype interaction (p<0.001), a significant main effect of phase (p<0.001), but no significant main effect of genotype (Figure 1f). In summary, relative to female WT littermates, female *Pcdh10*$^{+/-}$ mice did not show a significant alteration in social approach, but did show some evidence for reduced exploration of both cylinders in this test. A similar pattern of male-specific reduction in social approach behavior was found in time spent in the social and non-social chambers (see Supplementary Figure S1).

General exploration was largely not affected by Pcdh10 haploinsufficiency. Neither male nor female *Pcdh10*$^{+/-}$ mice showed alterations in anxiety-like behavior in the elevated zero maze test (Figure S3a and 3b). Female, but not male, *Pcdh10*$^{+/-}$ mice showed alterations in motor coordination in the rotarod test (Figure S3c and 3d). Specifically, female *Pcdh10*$^{+/-}$ mice, relative to female WT littermates, showed a slower rate of improvement in motor coordination across the trials (trial by genotype interaction p<0.001). There was no significant effect of genotype on olfactory functioning in males or females in the olfactory habituation-dishabituation test (Figure S4a and 4b). There was no significant effect of genotype on novel object recognition in males or females (Figure S5). Male *Pcdh10*$^{+/-}$ mice showed a reduction in rearing behavior, but there were no other significant genotype effects on repetitive behaviors in males or females (Figure S2). These data show reduced social approach and social sniffing behavior specifically in male *Pcdh10*$^{+/-}$ mice that is not attributable to deficits in exploratory behavior or olfactory function.

Pcdh10$^{+/-}$ pups exhibit increased frequency of ultrasonic vocalizations (USVs)

Relative to same-sex WT littermates, significantly increased numbers of USVs were seen in both male (p<0.001) and female (p<0.001) *Pcdh10*$^{+/-}$ mice (Figure 2) at postnatal day 6. Increased USVs are a dysregulation of communication that have been seen in pups of some other mouse models of ASD (32,51).

Reduced LA-BLA transmission of gamma frequency stimulation in brain slices from Pcdh10$^{+/-}$ mice

Impairments in social cognition and emotional processing observed in ASD and other neurodevelopmental disorders have been correlated with changes in functional connectivity and temporal binding of regional brain activity, particularly in the gamma frequency range (52–54). Social interaction in humans and rodents strongly engages amygdala circuits

including the basolateral amygdala, a brain region expressing high levels of PCDH10 (15,55,56). To determine whether functional connectivity is altered in amygdala circuitry of *Pcdh10*$^{+/-}$ male mice, voltage sensitive dye imaging was used to optically record the transmission of stimulation-evoked activity from lateral amygdala to its functional targets in basolateral amygdala and striatum in acute *ex vivo* slices from juvenile mice. The lateral amygdala was stimulated with a train of 4 stimuli at 40Hz to mimic gamma oscillatory input, and the spread of evoked changes in membrane potential in the basolateral amygdala (BLA) and nearby ventral caudate (STR) regions were imaged (Fig. 3a). No differences were found in the peak amplitude of responses in amygdala (Fig. 3c1) or striatal regions (Fig. 3c2), indicating no change in bulk synaptic transmission from the LA to BLA and STR. To test if high frequency activity can be reliably transmitted from the LA to these areas, the fluorescent response was convolved to measure power at the 40 Hz stimulus frequency. Measuring stimulus evoked power from *Pcdh10*$^{+/-}$ slices revealed a significant reduction in the power of BLA gamma band activity (Fig. 3e1, p=0.016), but no change in STR gamma band activity (Fig. 3e2). These results suggest that PCDH10 modulates synaptic and network connectivity in the BLA. We repeated this experiment in a separate set of slices in the absence and presence of d-cycloserine (dCS) 20 μM. dCS did not have a significant effect on gamma power in the BLA (data not shown).

Abnormal dendritic spines in lateral/basolateral amygdala of Pcdh10$^{+/-}$ males

Because Pcdh10 has been linked to spine elimination (17), we hypothesized that the behavioral deficits we observed may be related to an increase in spine density in the amygdala of *Pcdh10*$^{+/-}$ mice. By Golgi staining, no significant genotype effects were observed in the number of dendrites or branch points (Fig. 4c), but, as we had hypothesized, the dendritic spine density was increased in *Pcdh10*$^{+/-}$ neurons of the lateral and basolateral amygdala (LA/BLA) (Fig. 4d). When spines were categorized by morphological characteristics (36,37), we found that dendrites of *Pcdh10*$^{+/-}$ neurons contain a higher number of thin, elongated filopodia-like spines, an immature spine morphology, compared to dendrites of wild-type neurons (p=0.030) (Figure 4e, Figure S6) (37,57).

Decreased GluN1 and GluN2A in the PSD of amygdala of Pcdh10$^{+/-}$ male mice

Impaired social behavior and reduced gamma frequency responses have been described in mouse models with reduced NMDAR expression (58). We performed subcellular fractionation to obtain protein extracts enriched for synaptic and parasynaptic membranes and post-synaptic density (PSD), followed by Western blotting. Pcdh10 was highly concentrated in extracts enriched for PSD (Figure 5a). In PSD fractions from the amygdala, (Figure 5b and 5c), *Pcdh10*$^{+/-}$ mice showed significantly lower levels of Pcdh10 (p<0.001), GluN1 (p<0.001), and GluN2A (p=0.011) than WT. In PSD fractions from prefrontal cortex (PFC), there was no significant difference between *Pcdh10*$^{+/-}$ and WT mice in GluN1 or GluN2A levels, however Pcdh10 expression is relatively low in the PFC (data not shown) (15).

Rescue of social deficits in Pcdh10$^{+/-}$ male mice with NMDAR activation

One therapeutic agent that has shown promise in improving sociability in both animal models and human individuals with ASD is the NMDAR glycine site partial agonist d-

cycloserine (dCS) (59–61). Mice were treated with an acute, systemic injection of saline or dCS 30 min prior to social approach testing. The dose of dCS used – 32 mg/kg—is a moderate dose that enhances NMDA receptor function (59,62) and is a similar dose to that used in systemic injections to increase social approach behavior in another mouse model relevant to ASD (59). dCS rescued the deficit in social sniffing observed in *Pcdh10*+/− male mice (in phase 2, significant genotype by drug interaction, p=0.020) but did not alter non-social exploration or locomotor activity (Figure 6).

Discussion

Male mice lacking a single copy of *Pcdh10* exhibit atypical social approach and social communication behaviors, as well as altered structure and function of amygdala synaptic connections. *Pcdh10*$^{+/-}$ males do not show increased repetitive behaviors. The degree of social-communication and repetitive behavior symptoms are poorly correlated among humans with ASD (63), and the *Pcdh10*$^{+/-}$ model appears to be most relevant to social-communication behaviors.

Behavioral deficits in Pcdh10$^{+/-}$ male mice implicate amygdala dysfunction

Abnormal amygdala structure and function has been correlated with alterations in social behaviors in ASD and other neurodevelopmental disorders (16,53,64,65). Social interaction in humans and rodents strongly engages amygdala circuits including the BLA, which expresses high levels of PCDH10 (15,55,56). Juvenile male *Pcdh10*$^{+/-}$ mice exhibit impairments in social approach without alterations in general exploratory and anxiety-like behaviors.

Synaptic dysfunction in the amygdala of Pcdh10+/− males

Alterations in synaptic connections have been observed in the brains of individuals with ASD (7,66). LA/BLA neurons from adult male *Pcdh10*$^{+/-}$ mice have increased spine density, and that this largely reflects an increase in long filamentous processes. Increased spine density and extension of filopodia-like processes have been observed with manipulations that impair synaptic plasticity, synaptic transmission, or acutely block NMDAR activity (67–69). Dendrites with a dense covering of long, thin filopodia-type spines also have been described in adult neurons from individuals with Fragile X syndrome and in *Fmr1* KO mice (5,70). Loss of Fragile X protein FMRP disrupts trafficking and translational regulation of mRNAs encoding multiple synaptic structural and functional proteins, including *Protocadherin 10*. Pcdh10 is a functional target of FMRP that regulates spine elimination (17), suggesting that the increase in filopodia-like spines observed in the *Fmr1* KO may be attributed in part to reduced trafficking and function of Pcdh10. Elongation of spine necks is correlated with reduced charge transfer between spine head and the parent dendrite (71), suggesting that long filamentous spines are less effective at mediating synaptic transmission.

Behavioral and neuronal abnormalities in Pcdh10+/− mice are consistent with NMDAR dysfunction

Increasing evidence from studies of both human subjects and mouse models implicates NMDAR dysfunction in the pathophysiology of ASD (44). Genetic or pharmacological inhibition of NMDAR function disrupts social approach behavior and alters synchronized gamma activity in rodent models (45,58,72). In human subjects, reduction in NMDAR function and amygdala evoked gamma activity have been linked to impairment in emotional face processing (46,65,73). In juvenile *Pcdh10*$^{+/-}$ male mice, social approach deficits are accompanied by reduced synaptic NMDAR GluN1 and GluN2A subunits and impaired maintenance of the high-frequency gamma activity in the BLA, indicating that excitatory synaptic transmission and local circuit integrity are disrupted within this nucleus. Interestingly, acute enhancement of NMDAR function with the glycine site agonist dCS rescued the social approach deficit observed in these mice, suggesting that existing spines can be modified to rescue behavioral deficits. However, dCS applied to slices did not reverse the reduced BLA gamma band power phenotype, suggesting that the action of dCS on this isolated circuit on a slice – which lacks other inputs and outputs, as well as the behavior and experience of the awake behaving animal -- is not sufficient to explain the effect of systemic administration of dCS in rescuing social approach behavior.

Male bias is an important feature of ASD models

We show that a partial loss of Pcdh10 selectively impacts social approach behavior in male mice. ASD is more common in males than females (2,3). X-linked disorders, such as Fragile X, predictably show strong sex differences, but the majority of ASD-associated genes, including *Pcdh10*, are autosomal (9,74). These differences raise intriguing questions about the nature of sex differences, particularly in disorders with early, pre-pubertal onset (3). Organizational effects of the prenatal testosterone surge on the brains of male fetuses represent an early window for neuroendocrine effects on neural development and early social behavior (75,76). Interestingly, sex hormones modulate *Pcdh10* expression in non-neuronal tissue (77), suggesting a possible mechanism by which early hormone exposure may underlie sex specific effects in this model. Studies of their molecular and genetic underpinnings of sex differences in ASD models are important future directions, and will ultimately provide clues to mechanisms of vulnerability and resilience.

Supplementary Material

Refer to Web version on PubMed Central for supplementary material.

Acknowledgments

The authors wish to thank the following funding sources: Pennsylvania Department of Health (SAP # 4100042728) (R.T.S.), 1P50MH096891 (Raquel Gur)– subproject 6773 (E.S.B. and T.A.), National Institutes of Health Grants R01MH080718 (E.S.B.), ARRA supplement 3R01MH080718-03S1 (E.S.B.), The Sumitomo Foundation (S.H.), The Takeda Science Foundation (S.H.), JSPS KAKENHI Grant number 25430037(S.H.), MEXT-Supported Program for the Strategic Research Foundation at Private Universities S1201038 (S.H.), DFG International Research Training Group 1328 ‘Schizophrenia and Autism’ (H.S.), National Institute of Mental Health Training Program in Behavioral and Cognitive Neuroscience T32-MH017168 (H.S., T.A., D.F), the McMorris Autism Training Program (H.S. and S.F.), and National Institute of Neurological Disorders and Stroke Training Program in Neurodevelopmental Disabilities T32-NS007413 (S.F). The content is solely the responsibility of the authors and

does not necessarily represent the official views of the National Institutes of Health. The Pennsylvania Department of Health specifically disclaims responsibility for any analyses, interpretations, or conclusions. We thank Elena Mahrt and Christine Portfors (Washington State University) for guidance in methods for analyzing pup ultrasonic vocalizations.

References

1. Chevallier C, Kohls G, Troiani V, Brodkin ES, Schultz RT. The social motivation theory of autism. Trends in Cognitive Sciences. 2012:231–238. [PubMed: 22425667]
2. Werling DM, Geschwind DH. Sex differences in autism spectrum disorders. Curr Opin Neurol. 2013 Apr; 26(2):146–153. [PubMed: 23406909]
3. Hartley SL, Sikora DM. Sex differences in Autism spectrum disorder: An examination of developmental functioning, Autistic symptoms, and coexisting behavior problems in toddlers. J Autism Dev Disord. 2009 Dec; 39(12):1715–1722. [PubMed: 19582563]
4. Gilman SR, Iossifov I, Levy D, Ronemus M, Wigler M, Vitkup D. Rare De Novo Variants Associated with Autism Implicate a Large Functional Network of Genes Involved in Formation and Function of Synapses. Neuron. 2011; 70(5):898–907. [PubMed: 21658583]
5. Irwin SA, Patel B, Idupulapati M, Harris JB, Crisostomo RA, Larsen BP, et al. Abnormal dendritic spine characteristics in the temporal and visual cortices of patients with fragile-X syndrome: A quantitative examination. Am J Med Genet. 2001; 98(2):161–167. [PubMed: 11223852]
6. Wolff JJ, Gu H, Gerig G, Elison JT, Styner M, Gouttard S, et al. Differences in white matter fiber tract development present from 6 to 24 months in infants with autism. Am J Psychiatry. 2012; 169(16):589–600. [PubMed: 22362397]
7. Hutsler JJ, Zhang H. Increased dendritic spine densities on cortical projection neurons in autism spectrum disorders. Brain Res. 2010; 1309:83–94. [PubMed: 19896929]
8. Toro R, Konyukh M, Delorme R, Leblond C, Chaste P, Fauchereau F, et al. Key role for gene dosage and synaptic homeostasis in autism spectrum disorders. Trends Genet. 2010; 26(8):363–372. [PubMed: 20609491]
9. Morrow EM, Yoo S-Y, Flavell SW, Kim T-K, Lin Y, Hill RS, et al. Identifying autism loci and genes by tracing recent shared ancestry. Science. 2008; 321(5886):218–223. [PubMed: 18621663]
10. De Rubeis S, He X, Goldberg AP, Poultney CS, Samocha K, Ercument Cicek A, et al. Synaptic, transcriptional and chromatin genes disrupted in autism. Nature. 2014; 515(7526):209–215. [PubMed: 25363760]
11. O'Roak BJ, Vives L, Girirajan S, Karakoc E, Krumm N, Coe BP, et al. Sporadic autism exomes reveal a highly interconnected protein network of de novo mutations. Nature. 2012:246–250.
12. Kim SY, Yasuda S, Tanaka H, Yamagata K, Kim H. Non-clustered protocadherin. Cell Adhesion and Migration. 2011:97–105. [PubMed: 21173574]
13. Bucan M, Abrahams BS, Wang K, Glessner JT, Herman EI, Sonnenblick LI, et al. Genome-wide analyses of exonic copy number variants in a family-based study point to novel autism susceptibility genes. PLoS Genet. 2009; 5(6)
14. Hirano S, Yan Q, Suzuki ST. Expression of a novel protocadherin, OL-protocadherin, in a subset of functional systems of the developing mouse brain. J Neurosci. 1999; 19(3):995–1005. [PubMed: 9920663]
15. Aoki E, Kimura R, Suzuki ST, Hirano S. Distribution of OL-protocadherin protein in correlation with specific neural compartments and local circuits in the postnatal mouse brain. NeuroScience. 2003; 117(3):593–614. [PubMed: 12617965]
16. Kim JE, Lyoo IK, Estes AM, Renshaw PF, Shaw DW, Friedman SD, et al. Laterobasal amygdalar enlargement in 6- to 7-year-old children with autism spectrum disorder. Arch Gen Psychiatry. 2010; 67(11):1187–1197. [PubMed: 21041620]
17. Tsai N-P, Wilkerson JR, Guo W, Maksimova Ma, DeMartino GN, Cowan CW, et al. Multiple autism-linked genes mediate synapse elimination via proteasomal degradation of a synaptic scaffold PSD-95. Cell. Elsevier Inc. 2012 Dec 21; 151(7):1581–1594.

18. Dictenberg JB, Swanger Sa, Antar LN, Singer RH, Bassell GJ. A direct role for FMRP in activity-dependent dendritic mRNA transport links filopodial-spine morphogenesis to fragile X syndrome. Dev Cell. 2008 Jun; 14(6):926–939. [PubMed: 18539120]
19. Nakao S, Platek A, Hirano S, Takeichi M. Contact-dependent promotion of cell migration by the OL-protocadherin-Nap1 interaction. J Cell Biol. 2008; 182(2):395–410. [PubMed: 18644894]
20. Pilpel Y, Segal M. Rapid WAVE dynamics in dendritic spines of cultured hippocampal neurons is mediated by actin polymerization. J Neurochem. 2005 Dec; 95(5):1401–1410. [PubMed: 16190876]
21. DeRubeis S, Pasciuto E, Li K, Fernández E, DiMarino D, Buzzi A, et al. CYFIP1 coordinates mRNA translation and cytoskeleton remodeling to ensure proper dendritic spine formation. Neuron. 2013; 79:1169–1182. [PubMed: 24050404]
22. Uemura M, Nakao S, Suzuki ST, Takeichi M, Hirano S. OL-Protocadherin is essential for growth of striatal axons and thalamocortical projections. Nat Neurosci. 2007 Sep; 10(9):1151–1159. [PubMed: 17721516]
23. Fairless AH, Shah RY, Guthrie AJ, Li H, Brodkin ES. Deconstructing sociability, an autism-relevant phenotype, in mouse models. Anat Rec. 2011; 294(10):1713–1725.
24. Ehrlichman RS, Luminais SN, White SL, Rudnick ND, Ma N, Dow HC, et al. Neuregulin 1 transgenic mice display reduced mismatch negativity, contextual fear conditioning and social interactions. Brain Res. Elsevier B.V. 2009; 1294:116–127.
25. Tarantino LM, Gould TJ, Druhan JP, Bucan M. Behavior and mutagenesis screens: The importance of baseline analysis of inbred strains. Mamm Genome. 2000; 11(7):555–564. [PubMed: 10886023]
26. Yang M, Crawley JN. Simple behavioral assessment of mouse olfaction. Curr Protoc Neurosci. 2009; (SUPPL. 48)
27. Peça J, Feliciano C, Ting JT, Wang W, Wells MF, Venkatraman TN, et al. Shank3 mutant mice display autistic-like behaviours and striatal dysfunction. Nature. 2011 Apr 28; 472(7344):437–442. [PubMed: 21423165]
28. Tabuchi K, Blundell J, Etherton MR, Hammer RE, Liu X, Powell CM, et al. A neuroligin-3 mutation implicated in autism increases inhibitory synaptic transmission in mice. Science. 2007; 318(5847):71–76. [PubMed: 17823315]
29. Kwon CH, Luikart BW, Powell CM, Zhou J, Matheny SA, Zhang W, et al. Pten Regulates Neuronal Arborization and Social Interaction in Mice. Neuron. 2006; 50(3):377–388. [PubMed: 16675393]
30. Pietropaolo S, Guilleminot A, Martin B, D'Amato FR, Crusio WE. Genetic-background modulation of core and variable autistic-like symptoms in Fmr1 knock-out mice. PLoS One. 2011; 6(2)
31. Sala M, Braida D, Lentini D, Busnelli M, Bulgheroni E, Capurro V, et al. Pharmacologic rescue of impaired cognitive flexibility, social deficits, increased aggression, and seizure susceptibility in oxytocin receptor null mice: A neurobehavioral model of autism. Biol Psychiatry. 2011; 69(9): 875–882. [PubMed: 21306704]
32. Nakatani J, Tamada K, Hatanaka F, Ise S, Ohta H, Inoue K, et al. Abnormal Behavior in a Chromosome- Engineered Mouse Model for Human 15q11-13 Duplication Seen in Autism. Cell. 2009; 137(7):1235–1246. [PubMed: 19563756]
33. Hamilton SM, Spencer CM, Harrison WR, Yuva-Paylor LA, Graham DF, Daza RAM, et al. Multiple autism-like behaviors in a novel transgenic mouse model. Behav Brain Res. 2011; 218(1):29–41. [PubMed: 21093492]
34. Bidinosti M, Botta P, Kruttner S, Proenca CC, Stoehr N, Bernhard M, et al. CLK2 inhibition ameliorates autistic features associated with SHANK3 deficiency. 2016; 351(6278):1199–1203.
35. Branchi I, Santucci D, Alleva E. Ultrasonic vocalisation emitted by infant rodents: A tool for assessment of neurobehavioural development. Behavioural Brain Research. 2001:49–56.
36. Hering H, Sheng M. Dendritic spines: structure, dynamics and regulation. Nat Rev Neurosci. 2001; 2(12):880–888. [PubMed: 11733795]
37. Yuste R, Bonhoeffer T. Genesis of dendritic spines: insights from ultrastructural and imaging studies. Nat Rev Neurosci. 2004 Jan; 5(1):24–34. [PubMed: 14708001]

38. Carlson GC, Coulter DA. In vitro functional imaging in brain slices using fast voltage-sensitive dye imaging combined with whole-cell patch recording. Nat Protoc. 2008; 3(2):249–255. [PubMed: 18274527]
39. Oostenveld R, Fries P, Maris E, Schoffelen JM. FieldTrip: Open source software for advanced analysis of MEG, EEG, and invasive electrophysiological data. Comput Intell Neurosci. 2011; 2011
40. Gandal MJ, Edgar JC, Ehrlichman RS, Mehta M, Roberts TPL, Siegel SJ. Validating γ oscillations and delayed auditory responses as translational biomarkers of autism. Biol Psychiatry. 2010; 68(12):1100–1106. [PubMed: 21130222]
41. Hahn CG, Banerjee A, MacDonald ML, Cho DS, Kamins J, Nie Z, et al. The post-synaptic density of human postmortem brain tissues: An experimental study paradigm for neuropsychiatric illnesses. PLoS One. 2009; 4(4)
42. Banerjee, a; Wang, H-Y.; Borgmann-Winter, KE.; MacDonald, ML.; Kaprielian, H.; Stucky, A., et al. Src kinase as a mediator of convergent molecular abnormalities leading to NMDAR hypoactivity in schizophrenia. Mol Psychiatry. Nature Publishing Group. 2014 Oct-Aug;:1–10.
43. Fairless AH, Dow HC, Kreibich AS, Torre M, Kuruvilla M, Gordon E, et al. Sociability and brain development in BALB/cJ and C57BL/6J mice. Behav Brain Res. 2012; 228(2):299–310. [PubMed: 22178318]
44. Lee E-J, Choi SY, Kim E. NMDA receptor dysfunction in autism spectrum disorders. Curr Opin Pharmacol. Elsevier Ltd. 2015; 20:8–13.
45. Rung JP, Carlsson A, Markinhuhta KR, Carlsson ML. (+)-MK-801 induced social withdrawal in rats; A model for negative symptoms of schizophrenia. Prog Neuro-Psychopharmacology Biol Psychiatry. 2005; 29:827–832.
46. Wright B, Alderson-Day B, Prendergast G, Bennett S, Jordan J, Whitton C, et al. Gamma activation in young people with autism spectrum disorders and typically-developing controls when viewing emotions on faces. PLoS One. 2012 Jan.7(7):e41326. [PubMed: 22859975]
47. Verbeke G, Molenberghs G. Linear mixed models for longitudinal data. Springer series in statistics. 2000:568.
48. Gibbons RD, Hedeker D, Elkin I, et al. Some conceptual and statistical issues in analysis of longitudinal psychiatric data: Application to the nimh treatment of depression collaborative research program dataset. Arch Gen Psychiatry. 1993; 50(9):739–750. [PubMed: 8357299]
49. Fairless AH, Katz JM, Vijayvargiya N, Dow HC, Kreibich AS, Berrettini WH, et al. Development of home cage social behaviors in BALB/cJ vs. C57BL/6J mice. Behav Brain Res. Elsevier B.V. 2013 Jan.237:338–347.
50. Sankoorikal GMV, Kaercher Ka, Boon CJ, Lee JK, Brodkin ES. A mouse model system for genetic analysis of sociability: C57BL/6J versus BALB/cJ inbred mouse strains. Biol Psychiatry. 2006; 59:415–423. [PubMed: 16199013]
51. Scattoni ML, Gandhy SU, Ricceri L, Crawley JN. Unusual repertoire of vocalizations in the BTBR T+tf/J mouse model of autism. PLoS One. 2008; 3(8)
52. Wilson TW, Rojas DC, Reite ML, Teale PD, Rogers SJ. Children and adolescents with autism exhibit reduced MEG steady-state gamma responses. Biol Psychiatry. 2007 Aug 1; 62(3):192–197. [PubMed: 16950225]
53. Das P, Kemp AH, Flynn G, Harris AWF, Liddell BJ, Whitford TJ, et al. Functional disconnections in the direct and indirect amygdala pathways for fear processing in schizophrenia. Schizophr Res. 2007 Feb; 90(1-3):284–294. [PubMed: 17222539]
54. Supekar K, Uddin LQ, Khouzam A, Phillips J, Gaillard WD, Kenworthy LE, et al. Brain Hyperconnectivity in Children with Autism and its Links to Social Deficits. Cell Rep. 2013; 5(3): 738–747. [PubMed: 24210821]
55. Felix-Ortiz AC, Beyeler A, Seo C, Leppla Ca, Wildes CP, Tye KM. BLA to vHPC inputs modulate anxiety-related behaviors. Neuron. Elsevier Inc. 2013 Aug 21; 79(4):658–664.
56. Ferguson JN, Aldag JM, Insel TR, Young LJ. Oxytocin in the medial amygdala is essential for social recognition in the mouse. J Neurosci. 2001; 21(20):8278–8285. [PubMed: 11588199]
57. Ziv NE, Smith SJ. Evidence for a role of dendritic filopodia in synaptogenesis and spine formation. Neuron. 1996; 17:91–102. [PubMed: 8755481]

58. Gandal MJ, Sisti J, Klook K, Ortinski PI, Leitman V, Liang Y, et al. GABAB-mediated rescue of altered excitatory–inhibitory balance, gamma synchrony and behavioral deficits following constitutive NMDAR-hypofunction. Translational Psychiatry. 2012:e142. [PubMed: 22806213]
59. Won H, Lee H-R, Gee HY, Mah W, Kim J-I, Lee J, et al. Autistic-like social behaviour in Shank2-mutant mice improved by restoring NMDA receptor function. Nature [Internet]. Nature Publishing Group. 2012 Jun 14; 486(7402):261–265. [cited 2014 Oct 6] Available from: http://www.ncbi.nlm.nih.gov/pubmed/22699620.
60. Posey DJ, Kem DL, Swiezy NB, Sweeten TL, Wiegand RE, McDougle CJ. A pilot study of D-cycloserine in subjects with autistic disorder. Am J Psychiatry. 2004; 161(11):2115–2117. [PubMed: 15514414]
61. Burket JA, Benson AD, Tang AH, Deutsch SI. D-Cycloserine improves sociability in the BTBR T+ Itpr3tf/J mouse model of autism spectrum disorders with altered Ras/Raf/ERK1/2 signaling. Brain Res Bull. 2013; 96:62–70. [PubMed: 23685206]
62. Blundell J, Blaiss CA, Etherton MR, Espinosa F, Tabuchi K, Walz C, et al. Neuroligin-1 deletion results in impaired spatial memory and increased repetitive behavior. J Neurosci. 2010; 30(6): 2115–2129. [PubMed: 20147539]
63. Mandy WPL, Skuse DH. Research Review: What is the association between the social-communication element of autism and repetitive interests, behaviours and activities? Journal of Child Psychology and Psychiatry and Allied Disciplines. 2008:795–808.
64. Kleinhans NM, Richards T, Weaver K, Johnson LC, Greenson J, Dawson G, et al. Association between amygdala response to emotional faces and social anxiety in autism spectrum disorders. Neuropsychologia. Elsevier Ltd. 2010 Oct; 48(12):3665–3670.
65. Williams LM, Whitford TJ, Nagy M, Flynn G, Harris AWF, Silverstein SM, et al. Emotion-elicited gamma synchrony in patients with first-episode schizophrenia: A neural correlate of social cognition outcomes. J Psychiatry Neurosci. 2009; 34(3):303–313. [PubMed: 19568482]
66. Irwin, Sa; Galvez, R.; Greenough, WT. Dendritic spine structural anomalies in fragile-X mental retardation syndrome. Cereb Cortex. 2000; 10:1038–1044. [PubMed: 11007554]
67. Petrak LJ, Harris KM, Kirov Sa. Synaptogenesis on mature hippocampal dendrites occurs via filopodia and immature spines during blocked synaptic transmission. J Comp Neurol. 2005 Apr; 484(2):183–190. [PubMed: 15736233]
68. Lin SY, Constantine-Paton M. Suppression of sprouting: An early function of NMDA receptors in the absence of AMPA/kainate receptor activity. J Neurosci. 1998; 18(10):3725–3737. [PubMed: 9570803]
69. Chen Y, Wang Y, Ertürk A, Kallop D, Jiang Z, Weimer RM, et al. Activity-induced Nr4a1 regulates spine density and distribution pattern of excitatory synapses in pyramidal neurons. Neuron. Cell Press. 2014; 83(2):431–443.
70. Comery TA, Harris JB, Willems PJ, Oostra BA, Irwin SA, Weiler IJ, et al. Abnormal dendritic spines in fragile X knockout mice: maturation and pruning deficits. Proc Natl Acad Sci U S A. 1997; 94(10):5401–5404. [PubMed: 9144249]
71. Harris KM, Stevens JK. Dendritic spines of CA 1 pyramidal cells in the rat hippocampus: serial electron microscopy with reference to their biophysical characteristics. J Neurosci. 1989; 9(8): 2982–2997. [PubMed: 2769375]
72. Lazarewicz MT, Ehrlichman RS, Maxwell CR, Gandal MJ, Finkel LH, Siegel SJ. Ketamine modulates theta and gamma oscillations. J Cogn Neurosci. 2010; 22:1452–1464. [PubMed: 19583475]
73. Schmidt A, Kometer M, Bachmann R, Seifritz E, Vollenweider F. The NMDA antagonist ketamine and the 5-HT agonist psilocybin produce dissociable effects on structural encoding of emotional face expressions. Psychopharmacology (Berl). 2013; 225:227–239. [PubMed: 22836372]
74. State MW, Sestan N. The Emerging Biology of Autism Spectrum Disorders. Science. 2012:1301–1303.
75. Lutchmaya S, Baron-Cohen S, Raggatt P. Foetal testosterone and eye contact in 12-month-old human infants. Infant Behav Dev. 2002; 25:327–335.
76. Christine Knickmeyer R, Baron-Cohen S. Fetal testosterone and sex differences. Early Hum Dev. 2006 Dec; 82(12):755–760. [PubMed: 17084045]

77. Gong P, Madak-erdogan Z, Li J, Cheng J, Greenlief CM, Helferich W, et al. Transcriptomic analysis identifies gene networks regulated by estrogen receptor α (ER α) and ER β that control distinct effects of different botanical estrogens. Nucl Recept Signal. 2014; 12:1–13.

78. Mahrt EJ, Perkel DJ, Tong L, Rubel EW, Portfors CV. Engineered deafness reveals that mouse courtship vocalizations do not require auditory experience. J Neurosci. 2013; 33(13):5573–5583. [PubMed: 23536072]

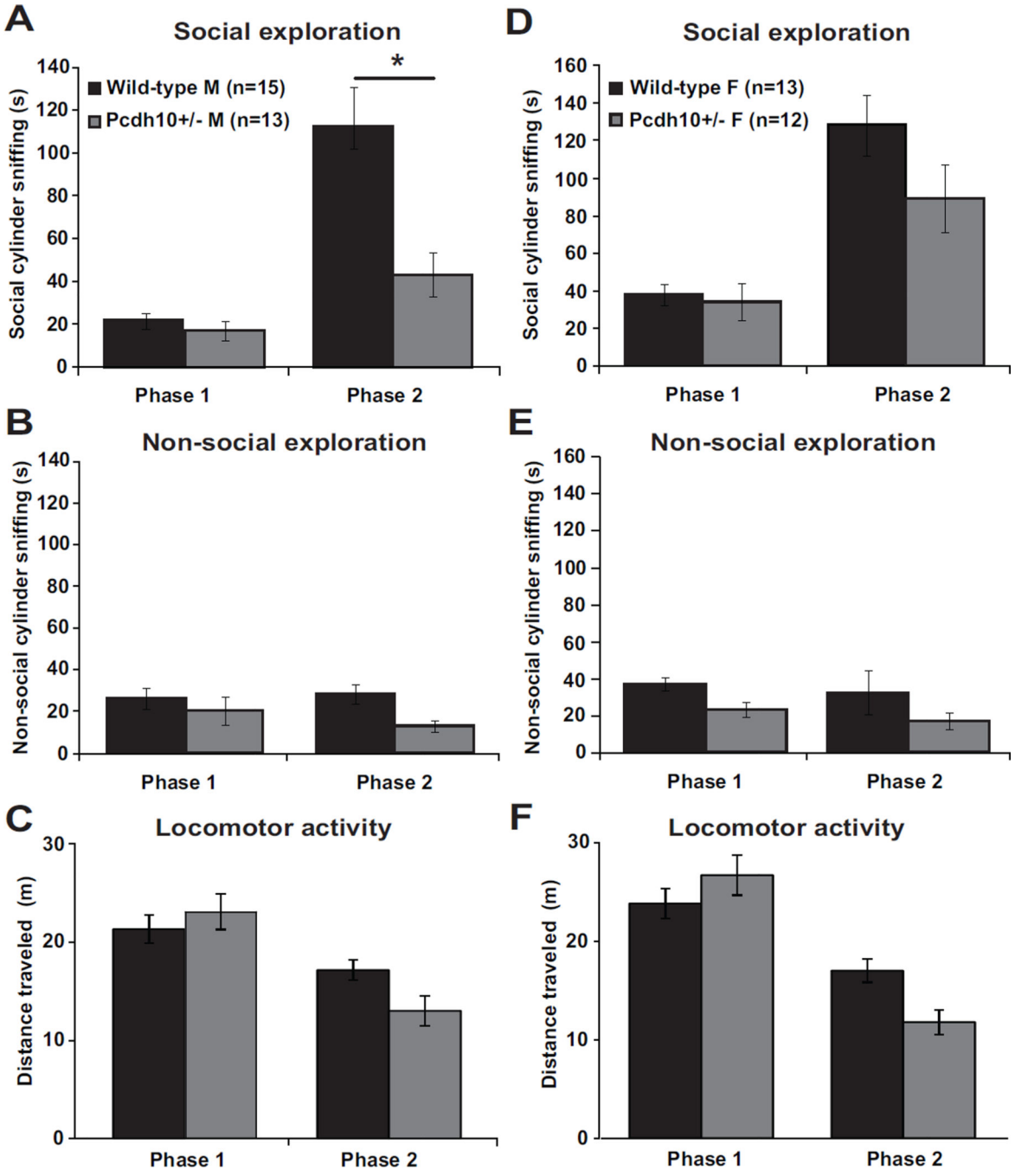

Figure 1. Reduced social approach behavior in juvenile *Pcdh10*$^{+/-}$ mice

a) Time spent sniffing the social cylinder in male *Pcdh10*$^{+/-}$ and WT littermates in Phase 1 (stimulus mouse absent) and Phase 2 (stimulus mouse present). The raw data are shown in the graph, but a log transformation was required for normality in order to carry out data analysis. Male *Pcdh10*$^{+/-}$ mice showed lower sociability, *i.e.*, significantly less increase in social cylinder sniffing duration from Phase 1 (absence of stimulus mouse) to Phase 2 (presence of stimulus mouse), than did male WT littermates (phase by genotype interaction, p=0.037, Figure 1a). There was a significant main effect of phase (p=0.001), but not a

significant main effect of genotype across both phases (p=0.067). **b)** Time spent sniffing the non-social cylinder (which was empty in Phase 1 and had an object in Phase 2) in male mice. The raw data are shown in the graph, but a log transformation was required for normality in order to carry out data analysis. There was no significant phase by genotype interaction (p=0.612), main effect of phase (p=0.238), or main effect of genotype (p=0.180). **c)** Distance traveled by male mice. There was a significant phase by genotype interaction (p<0.001), with a significant main effect of phase (p<0.001) but no significant main effect of genotype (p=0.121). **d)** Time spent sniffing the social cylinder in female *Pcdh10*$^{+/-}$ and WT littermates in Phase 1 and Phase 2. The raw data are shown in the graph, but a log transformation was required for normality in order to carry out data analysis. There was no significant phase by genotype interaction (p=0.583), but there was a main effect of phase (p=0.001) and a significant main effect of genotype across both phases (p=0.039). **e)** Time spent sniffing the nonsocial cylinder in female mice. The raw data are shown in the graph, but a log transformation was required for normality in order to carry out data analysis. There was no significant phase by genotype interaction (p=0.888), but there were significant main effects of phase (p=0.006) and genotype (p=0.022). **f)** Distance traveled by female mice. There was a significant phase by genotype interaction (p<0.001), a significant main effect of phase (p<0.001), but no significant main effect of genotype (p=0.167).

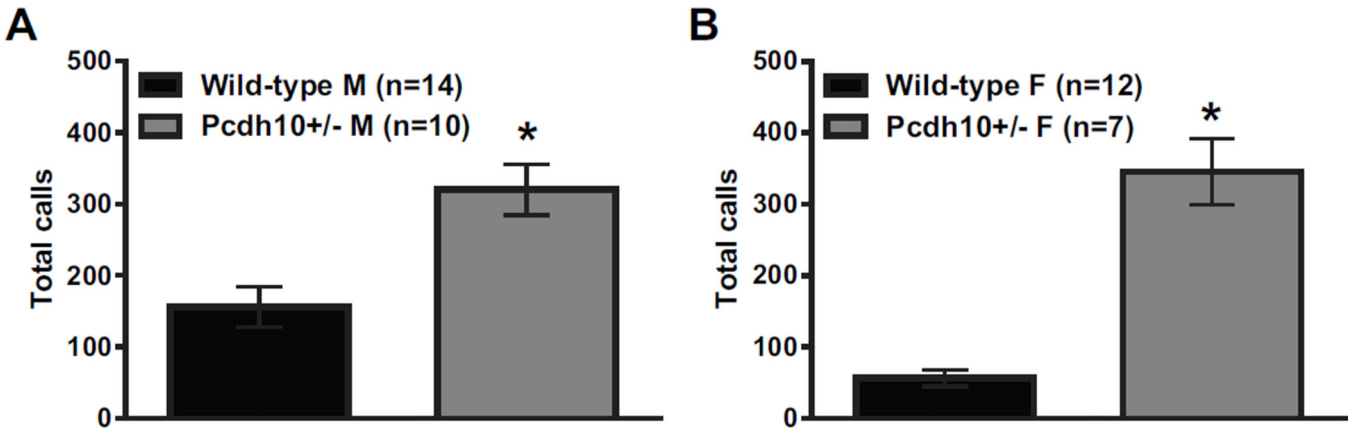

Figure 2. Increased ultrasonic vocalizations (USVs) in *Pcdh10*$^{+/-}$ pups

Analysis was performed in Avisoft SASLab Pro (version 5.2.09; Avisoft Bioacoustics) with the following settings: 1024 FFT length, 100% frame, Hamming window, 75% time window overlap, 15 and 500 kHz frequency cutoffs, amplitude threshold of −60 dB, and a hold time of 30ms (78). **a)** Male *Pcdh10*$^{+/-}$ mice showed significantly increased numbers of USVs relative to male WT littermates (effect of genotype $p<0.001$) over the 5min recording period on postnatal day 6. **b)** Female *Pcdh10*$^{+/-}$ mice also showed significantly increased numbers of USVs relative to female WT littermates (effect of genotype $p<0.001$) (Figure 2) over 5min.

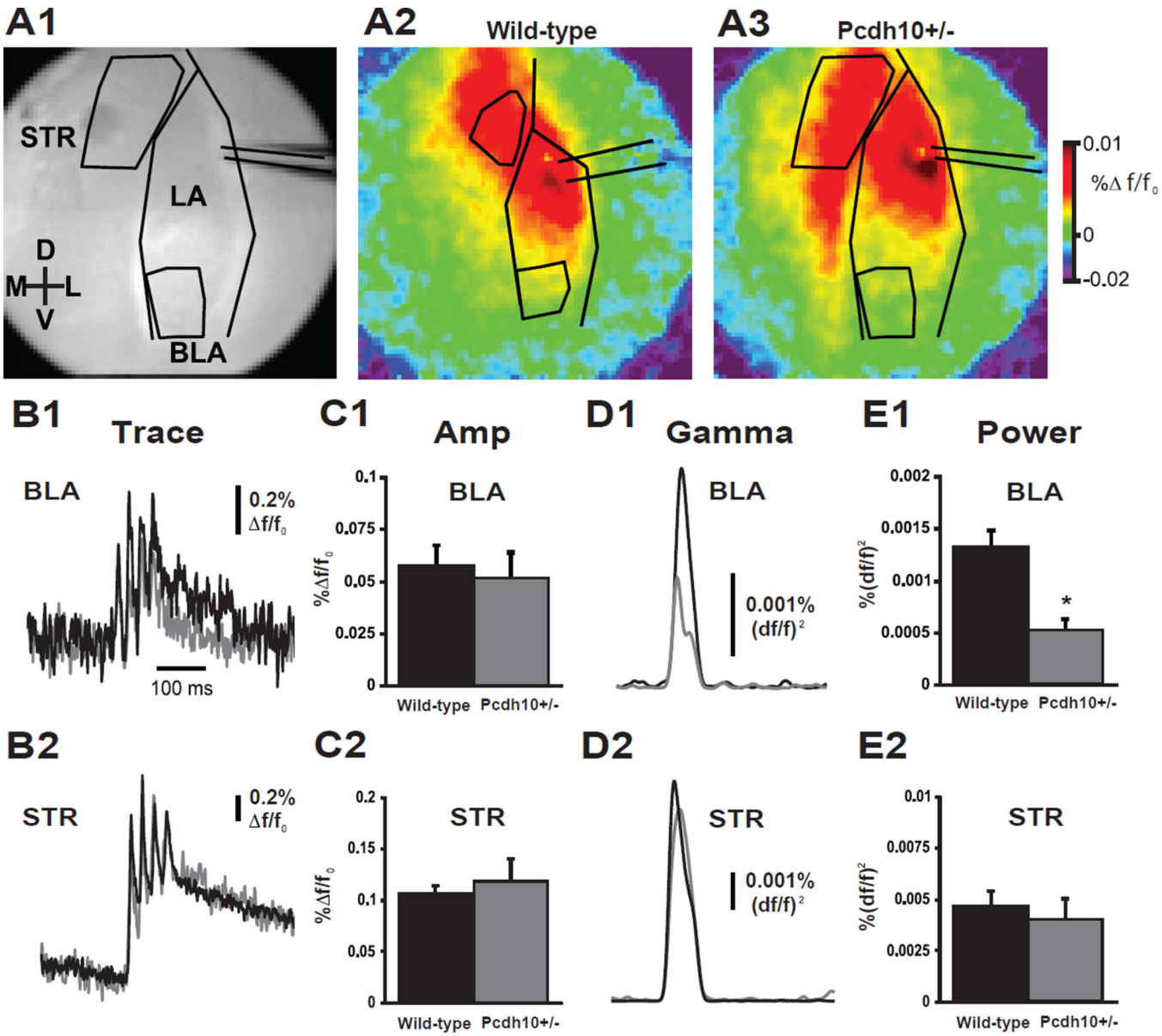

Figure 3. ***Pcdh10*$^{+/-}$ mice exhibit BLA-specific impairment for the transmission of gamma-band power, but not amplitude of EPSP**

a1) Grey scale image of amygdala coronal slice showing the lateral amygdala (LA), basolateral amygdala (BLA) and striatum (STR), electrode placement and regions of interest (ROI). Color images show peak VSDi responses following direct stimulation of the LA in slices from wild-type **(a2)** and *Pcdh10*$^{+/-}$ **(a3)** males. Data were displayed as the change in fluorescence divided by the resting fluorescence (Δf/f0). Depolarizing Δf/f0 signals were displayed as warmer colors and hyperpolarizations were represented as colder colors. Evoked average VSDi signal responses in the BLA **(b1)** and STR **(b2)** to 4 stimuli at 40Hz over time are shown. Traces from wild-type mice are shown in black and *Pcdh10*$^{+/-}$ are shown in gray. Statistical comparisons were made using a Mann-Whitney test. No differences were seen in the peak amplitude response in BLA **(c1)** or STR **(c2)** between wild-type and *Pcdh*$10^{+/-}$ (n=5; BLA, p=0.754; STR, p=0.754). In contrast, taking the

integral of the gamma-band response (30-50Hz) over time in both BLA **(d1)** and STR **(d2)** ROIs, revealed specific reduction in the gamma band coherence of the BLA in response to high frequency LA stimulation (BLA, p=0.016; STR p=0.917). This was specific to the LA - BLA circuit **(e1)**, as functional connectivity to the striatum **(e2)** remained unaffected.

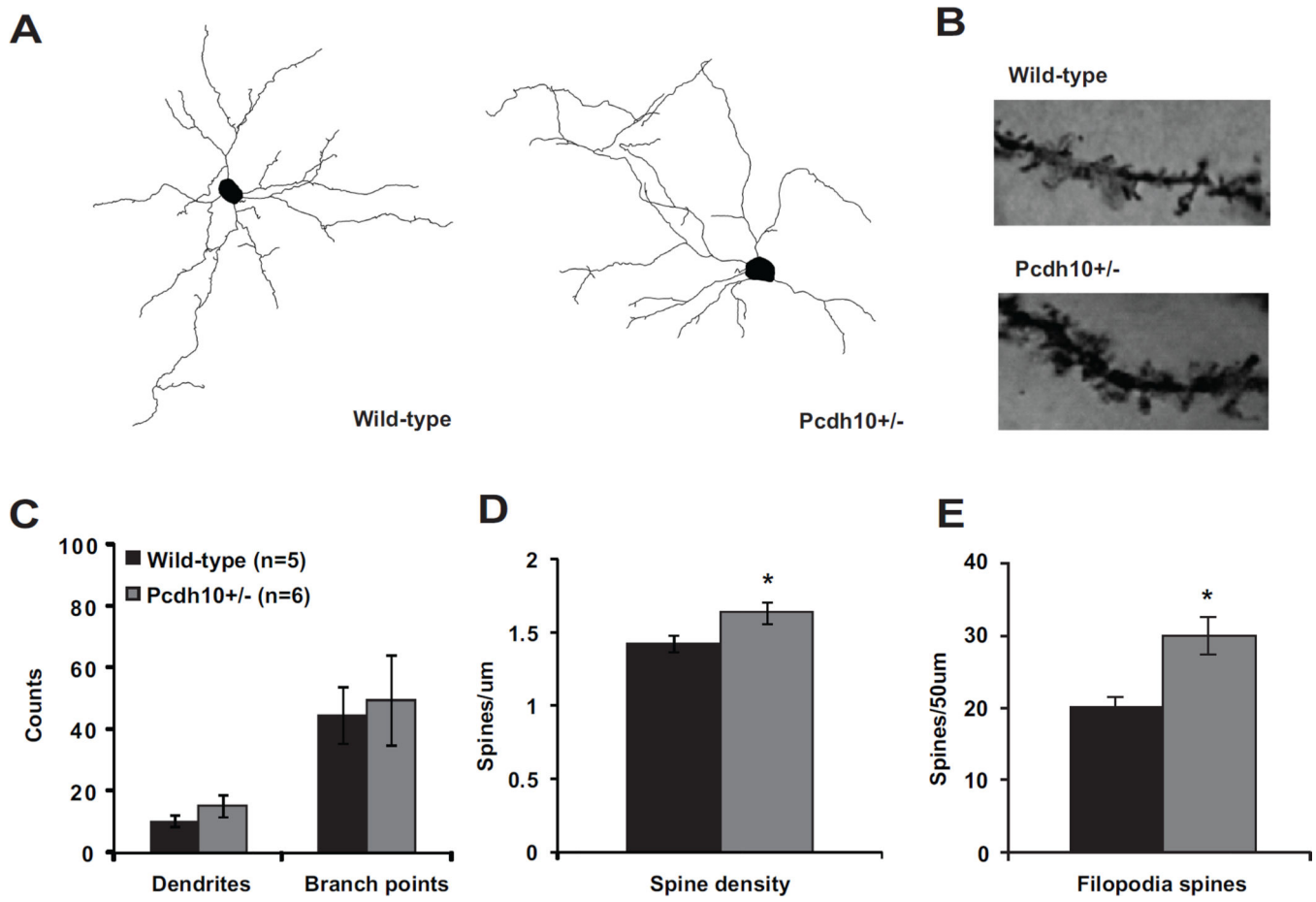

Figure 4. Increased filopodia-type spines on lateral/basolateral amygdala neurons of *Pcdh*10$^{+/-}$ males

a) Representative dendritic reconstructions from lateral/basolateral (LA/BLA) amygdala neurons from wild-type and *Pcdh*10$^{+/-}$ males. **b)** Representative dendritic lengths from LA/BLA neurons from wild-type and *Pcdh10*$^{+/-}$ males. **c)** Counts of dendrites and branch points in LA/BLA of wild-type and *Pcdh10*$^{+/-}$ males. A mixed model was used to compare the mean dendrites and branch points between the two genotypes, while considering the non-independence of multiple measurements within some mice. There was no difference in dendrites (p=0.190) or branch points (p=0.771) between the genotypes. **d)** A mixed model was used to compare the mean spine density in the LA/BLA between the two genotypes, while considering the non-independence of multiple measurements within some mice. Based on the available literature on the role of *Pcdh10* in spine elimination (17), a one-tailed test was applied to test our a priori directional hypothesis. Indeed, *Pcdh10*$^{+/-}$ mice had significantly higher spine density that WT littermates (p=0.048). **e)** A mixed model was fit separately for each spine type with a one-sided test, based on the a priori hypothesis of higher spine counts in *Pcdh10*$^{+/-}$ mice (17). Relative to WT, *Pcdh10*$^{+/-}$ amygdala neurons showed significantly higher levels of filopodia spines (p=0.030)

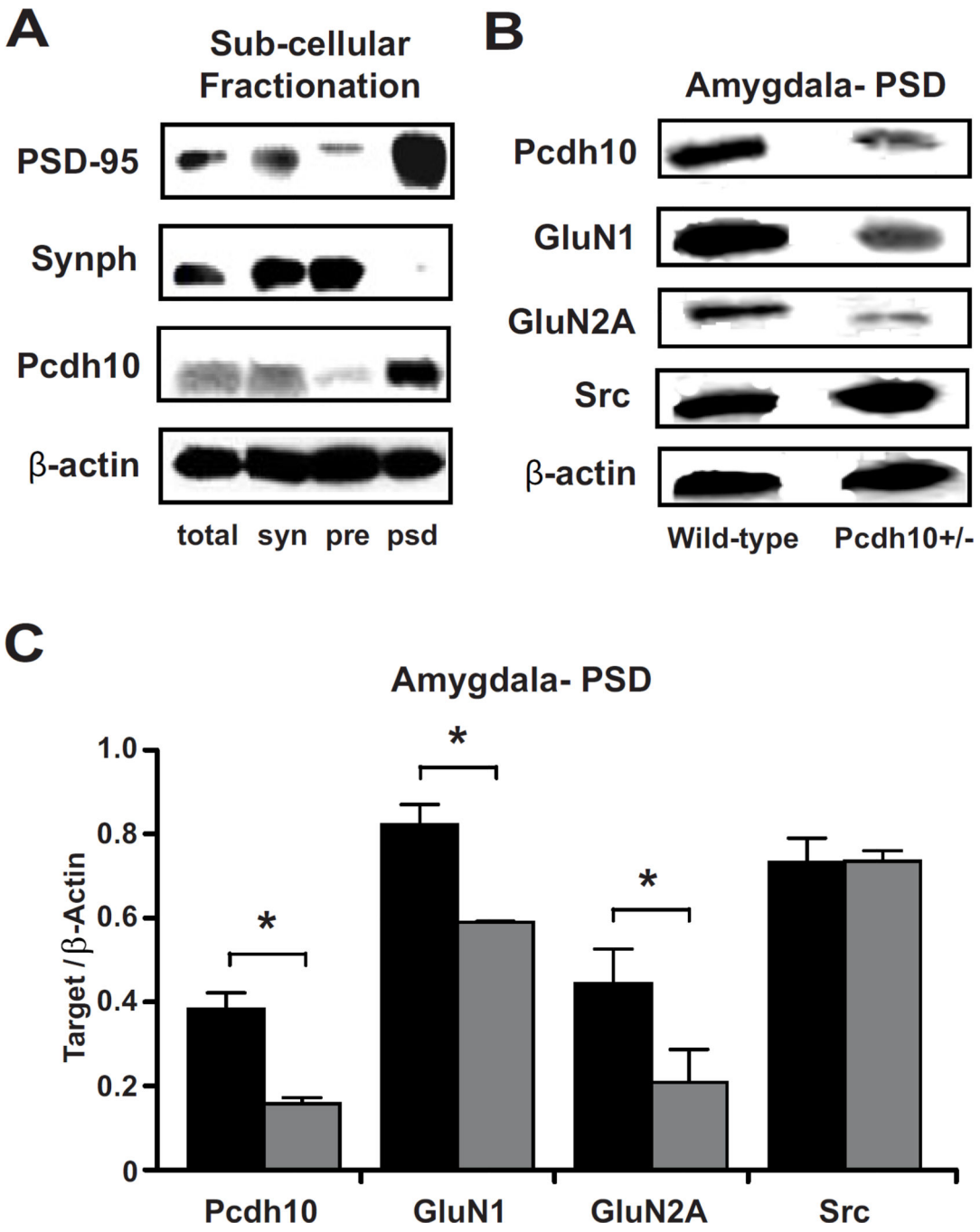

Figure 5. Decreased Pcdh10 in the PSD of *Pcdh*10$^{+/-}$ males was associated with decreased GLUN1 in the PSD

a) Pcdh10 was found to be concentrated in the post-synaptic density fraction (psd) where PSD-95, the marker for PSD is most concentrated; whereas it was found to be poorly represented in presynaptic fraction (pre) where Synaptophysin (Synph), the presynaptic marker, is heavily concentrated. **b)** Representative blots of Pcdh10, GluN1, GluN2A and β-actin in the PSD fractions of wild-type and *Pcdh10*$^{+/-}$ mice showing decreased Pcdh10, GluN1, and GluN2A in the amygdala of *Pcdh10*$^{+/-}$ mice. **c)** *Pcdh10*$^{+/-}$ mice showed

significantly reduced levels of Pcdh10 ($p<0.001$), GluN1 ($p<0.001$), and GluN2A ($p=0.011$), but not SRC ($p=0.939$).

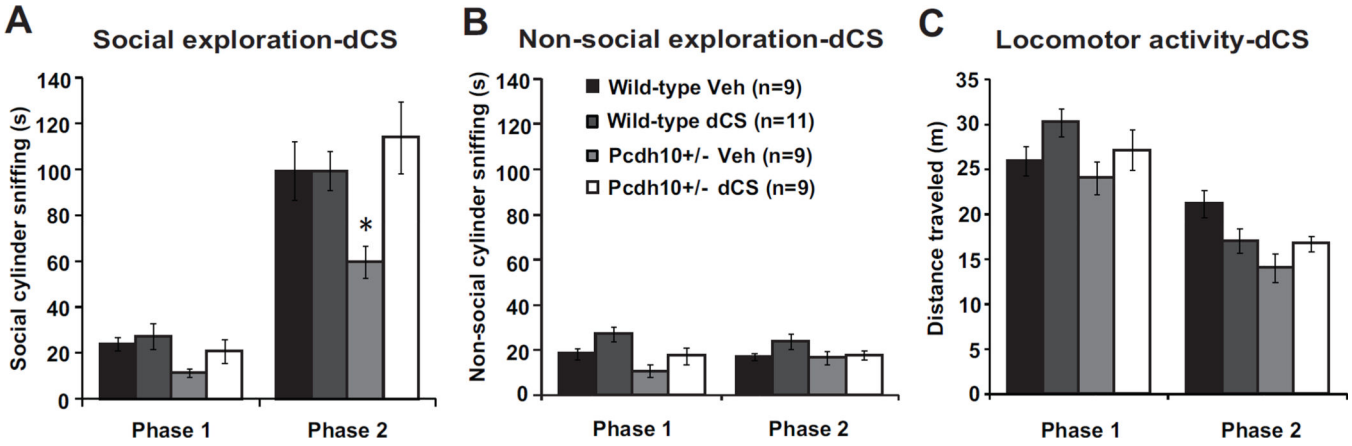

Figure 6. NMDAR agonist d-cycloserine rescued sociability impairment in *Pcdh10*$^{+/-}$ males

a) Treatment with acute d-cycloserine (dCS 32mg/kg) increased social exploration in juvenile *Pcdh*10$^{+/-}$ males. The raw data are shown in the graph, but a log transformation was required for normality in order to carry out data analysis. A mixed model was fit including the effects of phase (1,2), genotype (*Pcdh10*$^{+/-}$, WT), and drug (dCS, vehicle) on social cylinder sniffing. There was a significant phase by genotype interaction (p=0.020), but no other significant 2-way interactions. There were significant main effects of phase (p<0.001), genotype (p<0.001), and drug (p=0.019). To help interpret the genotype and drug effects, a separate model was fit for phase 2 only. In this model, there was a significant genotype by drug interaction (p=0.020) with significant main effects of genotype (p=0.006) and drug (p=0.001). **b)** Treatment with dCS and non-social cylinder sniffing. The raw data are shown in the graph, but a log transformation was required for normality in order to carry out data analysis. In a mixed model including phase, genotype, and drug, there was a significant phase by genotype interaction (p=0.020) but no other significant interactions. There were significant main effects of phase (p=0.009), genotype (p<0.001), and drug (p=0.026). To help interpret the genotype and drug effects, a separate model was fit for phase 2 only. In this model, there was no significant genotype by drug interaction (p=0.730) and no significant main effects of genotype (p=0.251) or drug (p=0.217). **c)** Treatment with dCS and distance traveled. In a mixed model including phase, genotype, and drug, there was a significant three-way interaction of phase by genotype by drug (p=0.046), but no significant two-way interactions. There was also a significant main effect of phase (p<0.001), but no main effects of genotype (p=0.386) or drug (0.158) on distance traveled. To help interpret the of genotype and drug effects, a separate model was fit for phase 2 only, which found a significant genotype by drug interaction (p=0.009) with a main effect of genotype (<0.001) but not drug (p=0.156).